23rd ABCM International Congress of Mechanical Engineering
December 6-11, 2015, Rio de Janeiro, RJ, Brazil

On the Sedimentation of a Blob of Particles Suspended in a Viscous Fluid

Wilber Cerqueira
Rafael Gabler Gontijo
Sara Malvar
Francisco Ricardo Cunha
University of Brasilia - Department of Mechanical Engineering - Vortex Group
rafaelgabler@gmail.com

Abstract. *This work explores the sedimentation process of an approximately initially spherical blob of dense particles immersed in a Newtonian fluid. We develop an experimental and numerical approach. For our experiments we designed a sedimentation column with super high viscosity silicon oil as the surrounding fluid. The particles are made of iron and sediment due to the action of gravity. The flow induced by the motion of the particles is in the Creeping flow regime, so we can reccur to fundamental laws of microhydrodynamics in order to compute numerically hydrodynamic interactions. We film the sedimentation process with a high definition camera and perform an image treatment analysis to count the main physical quantities of the problem. In this sense we account for the instant sedimentation velocity of the aggregate center of mass, the rate of particles escaping in the wake of the blob and the anisotropy ratio of the blob as a function of time. We also show some results obtained from numerical simulations developed by the authors with a non commercial academic research code called SIMS. For this purpose we use a sophisticated technique of Ewald sums in oder to account for particle hydrodynamic interactions in low Reynolds number flows. All the results obtained are interpreted from a physical perspective using scaling arguments and microstructural modifications to justify the alterations on the suspension transport properties. A good agreement is observed between our experiments, numerical simulations and scaling laws.*

Keywords: *Sedimentation, hydrodynamic interactions, particle wake, Ewald summation, particulate system.*

1. Introduction

Particulate wet systems are present in many industrial, biological and enviromental situations. The interest in understanding the physics of liquid-solid suspensions has attracted the interest of the scientific community since the early 1900's. For instance we can mention the work of Boycott (1920) that in the beggining of the XX century found out that an inclined channel may enhance the sedimentation speed of a dense solid inside a liquid. This effect is known as the Boycott (1920) effect. A great review over the physics of non Brownian liquid-solid suspensions is found at Davis and Acrivos (1985).

A remarkable feature of a non Colloidal liquid-solid suspension in the Creeping flow regime is the fact that even though the flow induced by the motion of a particle is governed by the Stokes equations (linear PDE's) the motion of a test particle confined in the middle of the suspension is highly nonlinear due to the interaction of the neighbouring particles. The effect of hydrodynamic interactions leads to a systematic decrease on the mean sedimentation velocity of the suspension as we increase the volume fraction of particles. Very good relations to predict this mean sedimentation velocity can be found in the works of Richardson and Zaki (1954), Hasimoto (1959), Batchelor (1972), Sangani and Acrivos (1982) and Brady-Durlofsky (1988).

We can also mention a very interesting numerical work done by Abade and Cunha (2007) where the authors investigated through numerical simulations the motion of a blob of particles sedimenting in a Newtonian viscous fluid. The author found out for example that the number of particles that escape from the main structure of the aggregate ΔN and remains on its wake is proportional to t^{-2} where t is the total time of the experiment. The problem is that the proportionality constant seems to be a function of the volume fraction of particles inside the blob and up to now there is no theory to compute this proportionality constant. One of the goals of this work is to investigate this relation through experiments.

The study of particulate wet systems of sedimenting spheres in Creeping flow presents many interesting branches. For instance we may use the kinematic reversibility principle for low Reynolds number flows, Kim and Karrila (2005), to study the physical mechanisms responsible for breaking the reversibility of particle trajectories. This study is important to understand not only the details of the micromechanics of dilute suspensions, Cunha and Hinch (1996), Cunha et al. (2013), but also to predict how long range particle interaction will induce velocity fluctuations in the system due to several different mechanisms.

For instance it is worthy to mention that we still have some interesting open question regarding the dynamic of sedimenting spheres in low Reynolds number flow. Even though we have a good understanding on the behavior of the mean sedimentation velocity of a random distributed suspension of hard spheres, we still face a paradox regarding the system variance. Caflisch and Luke (1985) have theoretically shown that the average variance of the system scales with its size, in this sense they found out that we would not be able to obtain a convergent value of the suspension mean variance. But the experiments of Nicolai and Guazzelli (1995) have obtained a convergent behavior of the suspension's mean variance with respect to its system size. This divergence has been observed also in the numerical works of Cunha et al. (2002), Ladd (2002) and Nguyen and Ladd (2004). One interesting fact is that both the numerical works mentioned have observed a screening in the behavior of the system's mean variance due to polidispersity effects. An interesting analysis of this problem is given by Hinch (1988).

The importance of understanding the micromechanics and microhydrodynamics in sedimentation is huge. This system has many possible applications in several fields of human knowledge. For instance with can metion geology, chemistry, engineering, physics, math, enviromental sciences, pharmaceutical industry and others. In many situations we are interested in speeding up the liquid-solid separation process that may be slowed down due to long range hydrodynamic interactions, Cunha et al. (2002). One possible way to increase the system average velocity is through the use of a magnetic suspension with a controlable magnetic field, as shown in the thesis of Gontijo (2013).

This brief introduction shows that there are still several chalenges in the deep understanding of low Reynolds number sedimentation, mainly due to the highly nonlinear behavior of individual particles influenced by the presence of neighbouring ones. In order to contribute for the production of a trusty experimental and numerical database, this work focus on a phenomenological description and analysis of the sedimentation proccess of an initially spherical sedimenting blob of dense iron particles immersed in a high viscosity transparent silicon oil. We film the motion of the blob and use video analysis techniques to obtain the main physical features of the system. We are interested in obtaining the behavior of the mean sedimentation velocity of the system as a function of time and in capturing topological modifications in the main structure of the blob such as shape distortion and particle escape in the wake region. Our experimental results are also compared with the non commercial research code SIMS developed by Gontijo (2013).

2. Numerical methodology

The numerical procedure to account the velocity of each particle considering hydrodynamic interactions is based on the work of Beenakker (1986). In this pionneer work, Beenakker (1986) used the Ewald (1921) summation technique applied to the Rotne-Prager (1969) mobility tensor to develop a numerically convergent summation technique capable to account for particle hydrodynamic interactions in a low Reynolds number flow. The developments of this technique are based on the fundamental theorems of microhydrodynamics and more details can be found on Gontijo (2013).

Since we are interested in studying the sedimentation proccess of a non Brownian supsension, we adopt velocity, length and time reference scales based on the Stokes velocity of an isolated particle $U_s = (2/9\eta)\Delta\rho g a^2$, where $\boldsymbol{u}^* = \boldsymbol{u}/U_s$, the radius of a single particle a, so $r^* = r/a$ and a convective time scale associated with the time that a particle sedimenting with the Stokes velocity takes in order to translate a distance equal to it's diameter, $t^* = tU_s/a$. Here the upper asterisks are used to denote dimentionless quantities. In order to simplify our notation from this moment dimentionless variables will be written in the same way as the dimentional variables in the last sections. Considering the characteristic velocity, length and time scales mentioned so far, the dimentionless system of equations that rule the motion of each α particle immersed in a viscous fluid and surrounded by several β particles is given by

$$\boldsymbol{u}_\alpha = \boldsymbol{M}^s_{\alpha,\alpha} \cdot \boldsymbol{f}_\alpha + \sum_{\beta \neq \alpha, \beta=1}^{N} \boldsymbol{M}^p_{\alpha,\beta} \cdot \boldsymbol{f}_\beta \tag{1}$$

with

$$\boldsymbol{f}_\alpha = \boldsymbol{f}^g_\alpha + \boldsymbol{f}^r_\alpha + \boldsymbol{f}^c_\alpha, \tag{2}$$

where $\boldsymbol{f}^g_\alpha$, $\boldsymbol{f}^r_\alpha$ and $\boldsymbol{f}^c_\alpha$ represent gravitational, respulsive (lubrication) and contact (Hertz) forces respectivelly. The dimentionless versions of the mobility matrices are expressed as

$$\boldsymbol{M}^s_{\alpha,\alpha} = \left(1 - 6\xi\pi^{-1/2} + \frac{40}{3}\xi^3\pi^{-1/2}\right)\boldsymbol{I}. \tag{3}$$

and

$$\boldsymbol{M}^{\alpha\beta}(\boldsymbol{r}') = \sum_{\boldsymbol{x}\in\mathcal{L}} \boldsymbol{M}^1(\boldsymbol{r}' + \boldsymbol{x}) + \frac{1}{V}\sum_{\boldsymbol{k}\in\hat{\mathcal{L}}, \boldsymbol{k}\neq 0} \boldsymbol{M}^2(\boldsymbol{k})\cos(\boldsymbol{k}\cdot\boldsymbol{r}'). \tag{4}$$

where the mobilities $\boldsymbol{M}^1$ and $\boldsymbol{M}^2$ are given by

$$\boldsymbol{M}^1(\boldsymbol{r}) = \frac{3}{4}\left\{\left(\frac{1}{r} + \frac{2}{3r^3}\right)\mathrm{erf}(\xi r) + \left(\frac{16}{3}\xi^7 r^4 + 4\xi^3 r^2 - \frac{80}{3}\xi^5 r^2 - 6\xi + \frac{56}{3}\xi^3 + \frac{4}{3}\xi r^2\right)\frac{1}{\sqrt{\pi}}\exp(-\xi^2 r^2)\right\}\boldsymbol{I}$$

$$+\frac{3}{4}\left\{\left(\frac{1}{r}-\frac{2}{r^3}\right)\mathrm{erfc}(\xi r)+\left(-\frac{16}{7}\xi^7 r^4-4\xi^3 r^2+\frac{64}{3}\xi^5 r^2+2\xi-\frac{8}{3}\xi^3-4\xi-4\xi\frac{1}{r^2}\right)\frac{1}{\sqrt{\pi}}\exp(\xi^2 r^2)\right\}\hat{\boldsymbol{r}}\hat{\boldsymbol{r}} \quad (5)$$

$$\boldsymbol{M}^2(\boldsymbol{k})=\left(\boldsymbol{I}-\hat{\boldsymbol{k}}\hat{\boldsymbol{k}}\right)\left(1-\frac{1}{3}k^2\right)\left(1+\frac{1}{4\xi^2}k^2+\frac{1}{8\xi^4}k^4\right)\frac{6\pi}{k^2}\exp\left(\frac{-k^2}{4\xi^2}\right), \quad (6)$$

where $\hat{\boldsymbol{k}}=\boldsymbol{k}/k$ e $\xi=\pi^{1/2}V^{-1/3}$. It is important to notice that the distance r and the parameter ξ expressed in equations (5 - 6) must be used in their dimentionless versions. The forces $\boldsymbol{f}_\alpha^g, \boldsymbol{f}_\alpha^r$ and $\boldsymbol{f}_\alpha^c$ necessary to calculate each particle velocity as expressed in (1) are given in their dimentionless versions as

$$\boldsymbol{f}_\alpha^g=-\hat{\boldsymbol{e}_z}, \quad \boldsymbol{f}_\alpha^r=\Lambda\,|\boldsymbol{u}_\alpha|\,e^{\left(-\frac{\epsilon_{\alpha\beta}}{\mathcal{Y}}\right)}\hat{\boldsymbol{e}}_r, \quad \boldsymbol{f}_\alpha^c=P_c\epsilon_{\alpha\beta}^{3/2}\hat{\boldsymbol{e}}_r, \quad (7)$$

here $\boldsymbol{e}_z$ is the positive direction of the z axis, parallel to gravity, Λ and $\mathcal{Y}$ are calibration constants of the model and P_c is a contact parameter, setted equal to $P_c=100$ in all the simulations of this work.

3. Experimental setup

To perform our experimets we used two Full High Definition digital cameras (Sony HDR-PJ230), a customized acrilic bench, a high performance computer and some video processing softwares (Matlab toolboxes and CVmob). A sketch of our experimental apparatus may be seen in Fig. 1. The fluid used in the experiments is the high viscosity silicon oil DMS-

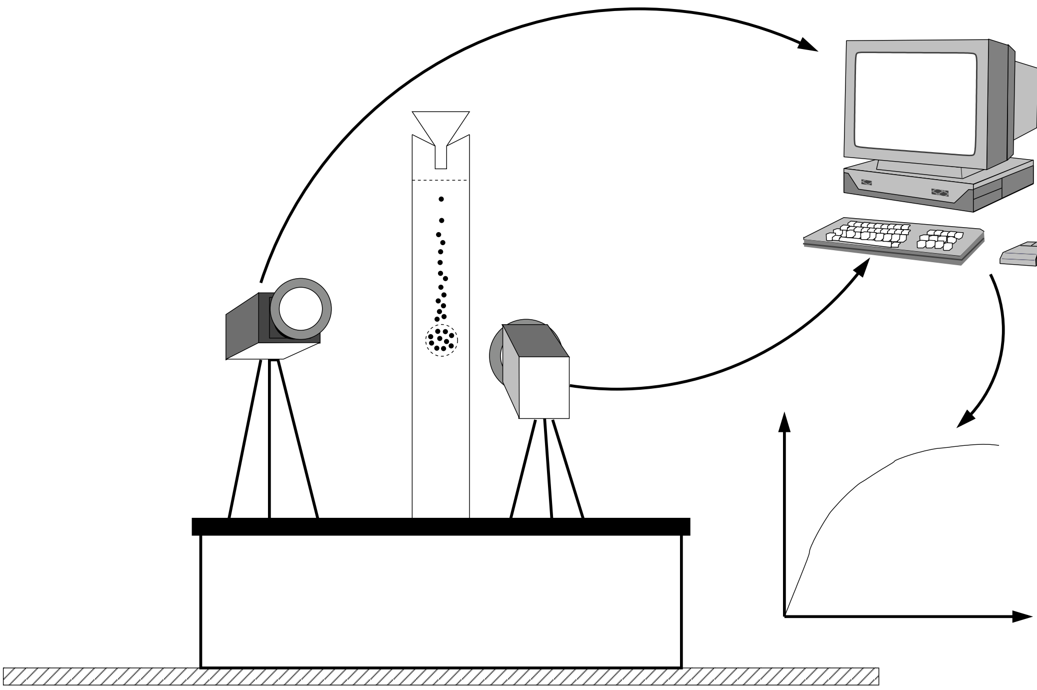

Figure 1: A sketch of our experimental setup. The videos recorded by two cameras positioned at different regions of the test section are sent to the computer. A video analysis is done in order to obtain the relevant informations of the problem.

60000. The particles used to form the spherical blob are iron particles with average diameter of $999.78\mu m \pm 110.45\mu m$ and mean density $\rho_s=7.92g/cm^3$. We performed a Stokes experiment to measure the fluid's viscosity and found out that the DMS-60000 has a viscosity of $\eta_f=64Pa.s$. The procedure to form a spherical blob is simple. We take a volume of $1ml$ of particles with a graduated cylinder and insert them inside a funnel at the top of the acrilic reservoir filled with silicon oil. The flow induced by the motion of the particles is within the low Reynolds number regime $Re_p \ll 1$, where Re_p represents the particle Reynolds number. In our experiments a typical particle Reynolds number is about $Re_p \sim 10^{-9}$. As the approximately initially spherical blob is formed we turn on two Full HD cameras at the same time but in different positions. These cameras are syncronized through a buzzer that produces a specific noise captured by their microphones at the same time. The option of filming with two cameras is important to make sure we are not loosing significant three dimentional information. These videos are recorded and analysed in a computer software. Here we have used the software CVmob to explored the motion of the aggregate. The informations of our analysis are: the mean sedimentation velocity of the spherical blob, its distortion with time and the rate of particles that escape through the wake of the aggregate due to hydrodynamic interactions and the backflow effect. All these informations may be availed through the mentioned software. We also made the characterization of the fluid through a Stokes experiment in order to measure its viscosity. The distribution of particles was obtained through an optical microscopy system. The details of the experimental apparatus used for the fluid and particles characterization are given next.

3.1 Characterization of the carrier liquid

In order to measure the DMS 60.000 viscosity we perform the Stokes experiment. From Stokes's law we obtain the terminal velocity for a spherical, smooth, rigid particle sedimenting in a viscous fluid in the limit of $Re \ll 1$, given by

$$V_s = \frac{2}{9}\frac{r^2 g(\rho_p - \rho_f)}{\eta} \tag{8}$$

where V_s is the sphere's terminal velocity, ρ_p is the density of the particle, ρ_f is the density of the fluid, r denotes the radius of the sphere, g is the magnitude of the gravitational acceleration vector and η is the dynamic viscosity of the fluid. By measuring ρ_p, ρ_f, r and V_s we can then isolate η and quantify the fluid's viscosity.

The experimental apparatus used for this purpose consists in a glass sphere, a digital scale to measure its mass, an Olympus UC 30 microscope to measure its diameter and seek for imperfections on the surface of the sphere, a prismatic box filled with 5 liters of silicone oil DMS 60.000 where the sphere is left to sediment, a Full HD digital camera to film its motion, a computer software (CVmob) to measure (from the movie) the sphere terminal velocity and a notebook.

Using an optical microscope, we checked for any imperfections on the surface of the sphere. Such imperfections may lead to lateral movements of the sphere in the silicone oil glass. These lateral movements are associated with asymmetric long range hydrodynamic interactions in low Reynolds number due to the presence of physical walls with different horizontal separations from the surface of the sphere. It is very important to use a smooth sphere to measure the viscosity of a fluid using the Stokes's experiment. Small superficial roughness in the sedimenting sphere may induce great deviations on our measures. For instance Cunha and Hinch (1996) has shown that a relation of $\epsilon/D \approx 10^{-4}$, where ϵ is the average roughness of the sphere and D is its diameter, may break the kinematic reversibility of a sedimenting sphere in low Reynolds number flow.

Figure 2 shows two images with $50\times$ and $200\times$ respective ampliations on the glass sphere used in our Stokes experiment. For this experiment we used a glass sphere with density $\rho_p = 2483.4[kg]/[m^3]$, immersed in a silicone oil with density $\rho_f = 970[kg]/[m^3]$, the sphere had a diameter $D = 4.7[mm]$, mass $m = 0.1350[g]$ and relative roughness $\epsilon/D = 2 \times 10^{-4}$. The terminal velocity that the sphere reaches was used with the Stokes's law to measure the fluid viscosity. This velocity was measured using the software CVmob that, through a video, follows the motion of the particle and provides its terminal velocity. Finally with all the informations, we are able to apply the Stokes's law and conclude that the viscosity (experimental) of the silicone oil used fluid is 64000 [cp] or 64 [Pa x s].

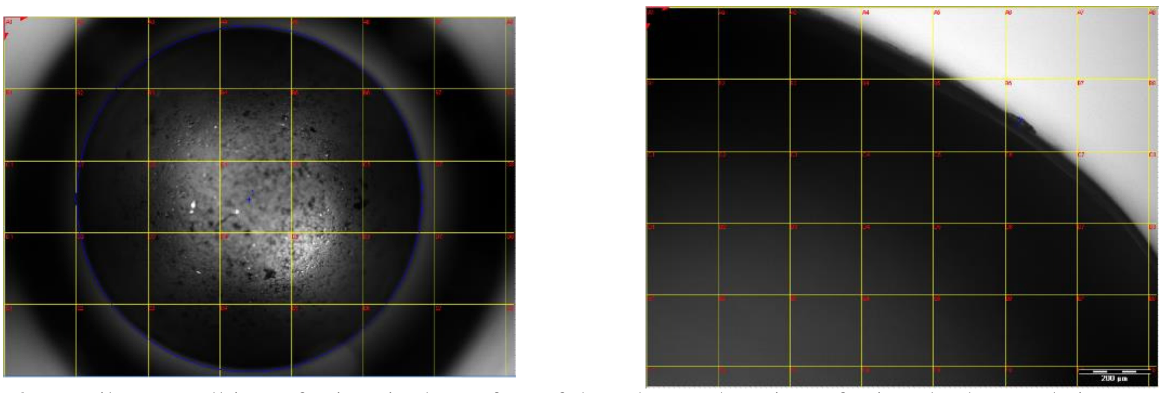

Figure 2: Details on small imperfections in the surface of the sphere. These imperfections lead to a relative roughness $\epsilon/D = 2 \times 10^{-4}$.

3.2 Characterization of the particulate phase

For our sedimentation experiment we have used small iron particles to create an approximately initially spherical blob that sediments on a high viscosity silione oil. The characterization of the particulate phase was done through a microscopy system. The results of our analysis are shown in Fig. 3.

We have used an optical microscope to count and measure the diameter of each particle in a sample. Using the minimum ampliation lens ($50\times$) we could only see about 20 particles in the microscope. We have then defined that each set of 5 samples containing 20 particles would be considered as 1 sample in our statistics. With this goal in mind we show the behavior of the acumulated average diameter d_m of our particles as a function of the number of samples. For this purpose we considered 25 samples of 100 particles, accounting for 2500 particles for this statistics. The same procedure was adopted to study the statistical behavior of the acumulated standard deviation Δ_d of the particles diameter. From Figs. 3a and 3b it is clear that both statistical quantities saturate for a number of samples equal to 15. The average of the last three values is indicated in the horizontal dashed line. The greatest difference between the average of the last three

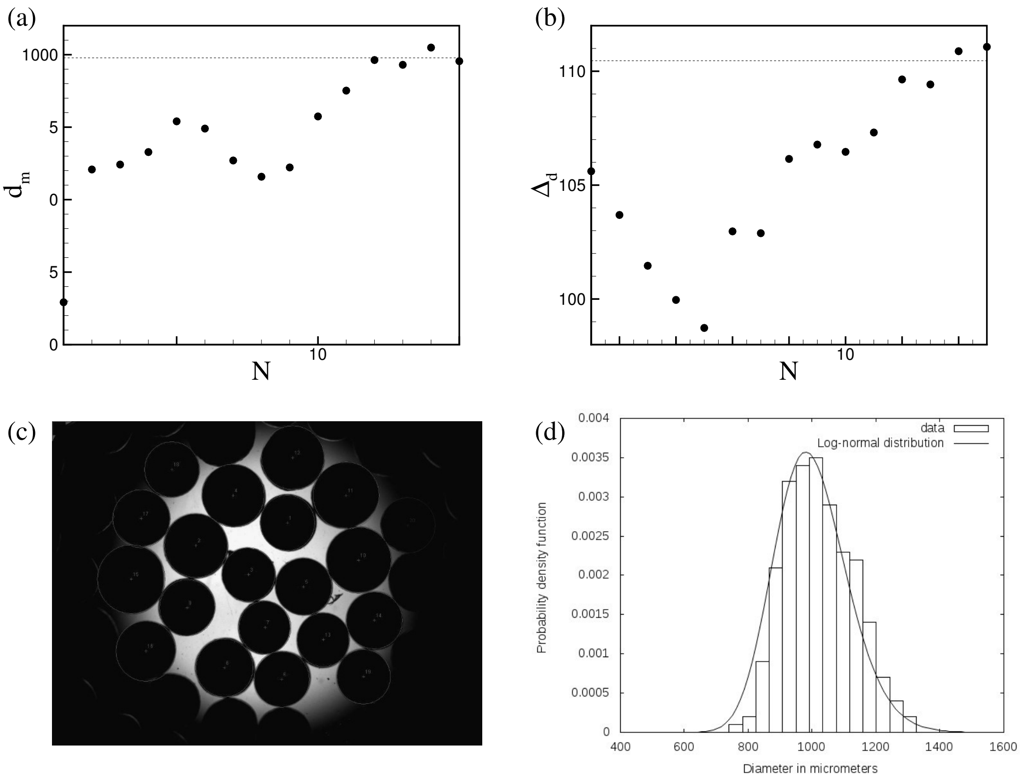

Figure 3: Figure (a) shows a plot of the acumulated average d_m diameter as a function of the number of samples. Figure (b) shows a plot of the acumulated standard deviation Δ_d of the particles diameter as a function of the number of samples analysed. Figure (c) illustrates a typical sample of 20 particles marked and measured by the microscopy system software analysis. Figure (d) shows the probability distribution function as a function of the diameters, the distribution is well fitted by a log-Normal distribution.

values and the acumulated average of a number of samples equal to 25 is lower than 1%. In this sense we may say that we have a meaningful statistics regarding the characterization of the particulate phase used in our experiments. The average diameter of the particles used in our experiment is $999.78\mu m \pm 110.45\mu m$. The probability distribution function of the particles diameter is well fitted by a log Normal distribution.

4. Results and discussions

First we show in Fig. 4 a typical sequence of the sedimentation process of the blob. These pictures were obtained experimentally. In Fig. 4 we highlight the edges of the falling blob in order to illustrate its shape deformation through the sedimentation process. It is possible to notice that the nearly initially isotropic structure deforms through the process. Thus it is observed a trace of escaping particles in the wake of the blob. These particles escape from the blob due to hydrodynamic interactions inside the aggregate that lead to velocity fluctuations. These fluctuations tend to throw the particles to the outside region of the blob. These particles are then captured by the backflow effect and end up being dragged to the wake of the blob.

Another qualitative analysis of the problem is shown in Fig. 5. In this picture we compare a numerical view of the aggregate strucutre after 12 Stokes time of simulation with a typical experiment run in the laboratory. In both pictures we have a total of $N = 1520$ particles. The volume fraction of particles inside the blob is $\phi_A = 1.2\%$.

We observe in both cases (numerical and experiment) a significant distortion on the blob shape induced by hydrodynamic interactions. In both cases it is also clear the formation of a deterministic trace of escaping particles at the wake of the blob. One interesting observation in Figs. 5a and 5b is the tendency of forming other smaller aggregates on the front of the blob. This phenomenon is clear in the numerical results. In the experiment we have the presence of physical walls at the bottom of the column and thus the lower wall tends to push the particles against the direction of gravity in an *action-reaction* mechanism. The hydrodynamic forces between the lower wall and the particles in the front of the aggregate tend to inhibit the formation of smaller aggregates in its front edge. It is important to say that our numerical/experimental comparisions must be done more in a qualitative manner, since we assume important restrictive assumptions in order to develop our numerical code. For instance we consider at the simulations a monodisperse suspension of perfectly spherical

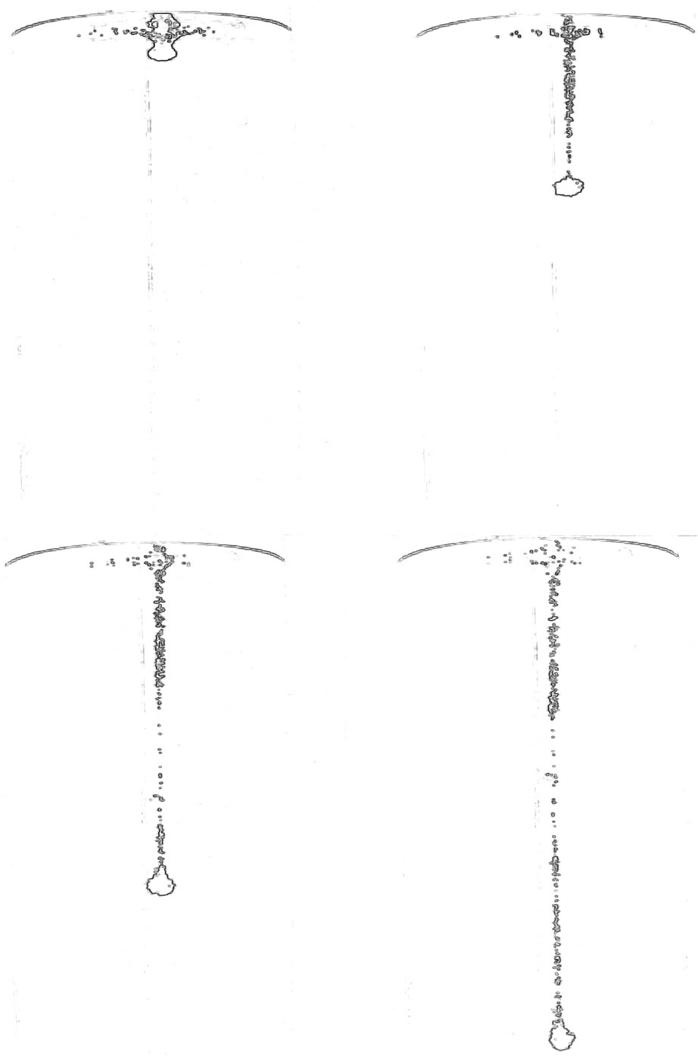

Figure 4: From upper left to lower right we show a typical sequence of the sedimentation proccess for an initially spherical blob.

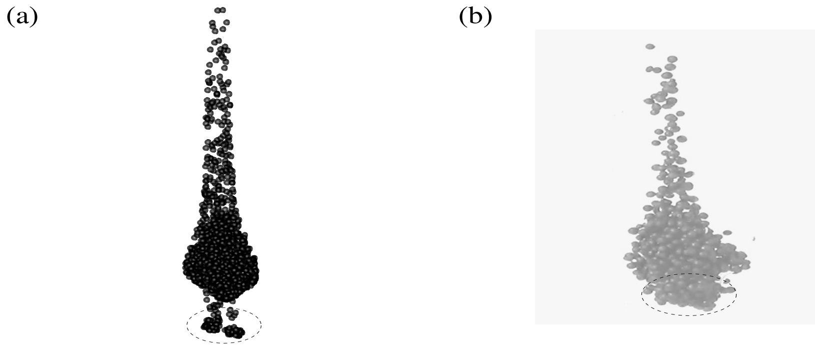

Figure 5: In (a) we show a typical structure after 12 Stokes time obtained numerically. In (b) we show the same structure obtained experimentally.

particles. However we have shown that the particles used in the experiments present a standard deviation of $11.74\%\ d_m$. In the experiments we also have the presence of physical walls that lead to important hydrodynamic interactions. These interactions may change the observed behavior when compared with a case of an infinit quiescent medium.

Figure 6 shows the dimensionless sedimentation velocity U/U_s of the aggregate center of mass (in the direction of gravity) as a function of time. We show a comparision between the experimental values with numerical data obtained from our numerical simulations. It is observed from Fig. 6 that in both situations (simulation and experiment) the average sedimentation velocity lies around the interval $49 \leq U_z \leq 57$. Even considering a monodisperse set of spherical particles in the numerical case, the deviation between the numerical average sedimentation velocity and its experimental correspondent is about $\Delta e \approx 10\%$.

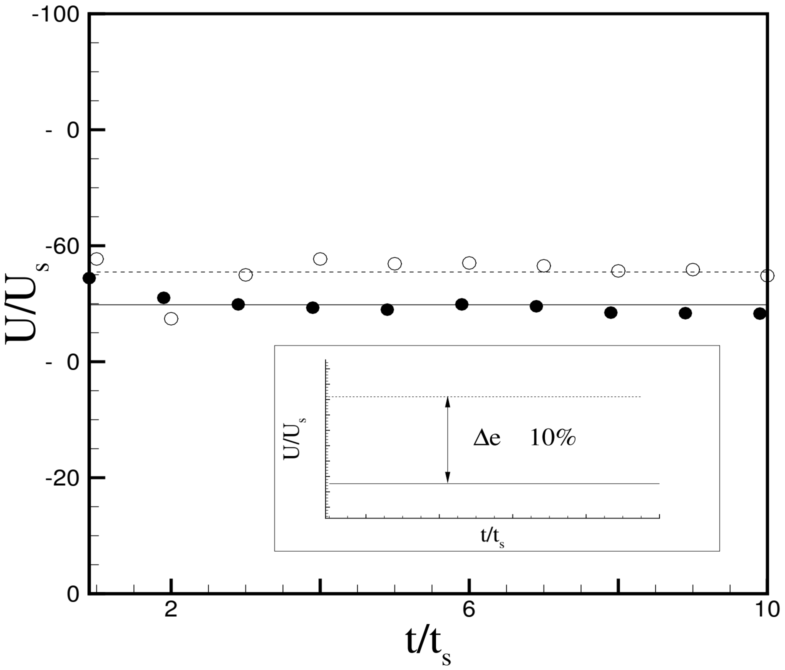

Figure 6: Sedimentation velocity on the direction of gravity U_z of the blob center of mass as a function of time t. The blank circles represent experimental values while the filled circles represent the numerical results. The continous line denotes the average numerical value while the dashed line represents the average experimental value.

If we make a simple balance between the blob's weight and drag forces in the creeping flow regime we have

$$|\boldsymbol{f}_g| = |\boldsymbol{f}_d| \tag{9}$$

being $|\boldsymbol{f}_g|$ the magnitude of the blob's net weight force (weight minus buoyancy) and $|\boldsymbol{f}_d|$ the magnitude of viscous forces acting on the aggregate. We have that $|\boldsymbol{f}_g| = N v_p \Delta\rho g$ and $|\boldsymbol{f}_d| = 6\pi\mu R_a U_a$, so

$$N v_p \rho_s g = 6\pi\mu R_a U_a \rightarrow U_a = \frac{N v_p \rho_s g}{6\pi\mu R_a} \rightarrow U_a = U_s \phi_A \left(\frac{R_a}{a}\right)^2, \tag{10}$$

where N is the number of particles inside the blob, v_p is thew volume of a single particle, $\Delta\rho$ is the density difference between the particles and the carrier liquid, g is the magnitude of gravity acceleration, R_a is the blob's radius, U_a is the sedimentation velocity of the blob, ϕ_A denotes the volume fraction of particles inside the blob and a is the radius of a single particle. Since the radius of the aggregate is much larger than the radius of an isolated particle ($R_a \gg a$), the blob sedimentation velocity is expected to be much larger than the Stokes velocity of an isolated particle. In this work for a volume fraction of particles inside the aggregate of $\phi_A = 1.2\%$ we have found that the average experimental value is $\overline{U/U_s}|_e = 55$ and the average numerical value is $\overline{U/U_s}|_n = 49$.

An important qualitative phenomenon shown in Figs. 4 and 5 is the systematic particle escape from the aggregate, induced by internal hydrodynamic interactions within the blob. In order to quantify the amount of particles that have escaped from the aggregate we show Fig. 7. In this figure we account for the number ΔN of particles that escaped from the main structure of the aggregate as a function of time. The results are presented in their non dimensional form. We use for comparision purposes an interesting scaling law obtained by Abade and Cunha (2007) which gives us the following relation

$$\Delta N \sim N_0 \left[1 - \frac{1}{(1+\kappa t)^2}\right], \quad \text{where} \;\; \kappa \sim \frac{3}{8}\sqrt{N_0}\epsilon^2, \tag{11}$$

where N_0 is the initial number of particles, κ is a constant related to the intensity of velocity fluctuations inside the blob, t is time and ϵ^2 is the area perpendicular to the direction of gravity that concentrates the region of the wake.

We have defined three regions in Fig. 7. Region **I** represents the beggining of the sedimentation process. A significant devition between the scaling law and the experimental values is observed. This deviation occurs due to the generation of the initial condition. It is virtually impossible to generate a perfect isotropic configuration in the laboratory. The attempt to produce an initially isotropic structure in the laboratory ends up releasing some particles. That is the reason for the observed deviation at region **I** in Fig. 7. A detail of the initial condition is shown in the insert of Fig. 7. Region **II** shows a good agreement between the scaling law of Abade and Cunha (2007) and our experiments. For a longer period of time the uncertanties in the counting of escaping particles increase and another deviation is observed in region **III**. We speculate that these uncertanties are related to the counting procedure that uses a two dimensional view from a video to count the particles. Even using two cameras to avoid the loss of information in different planes the probability of misscounting a particle increases with the number of particles in the wake. The deviation at region **III** suggests that further improvement must be done in the counting procedure. The constant κ used in equation (11) to fit the experimental behavior shown in

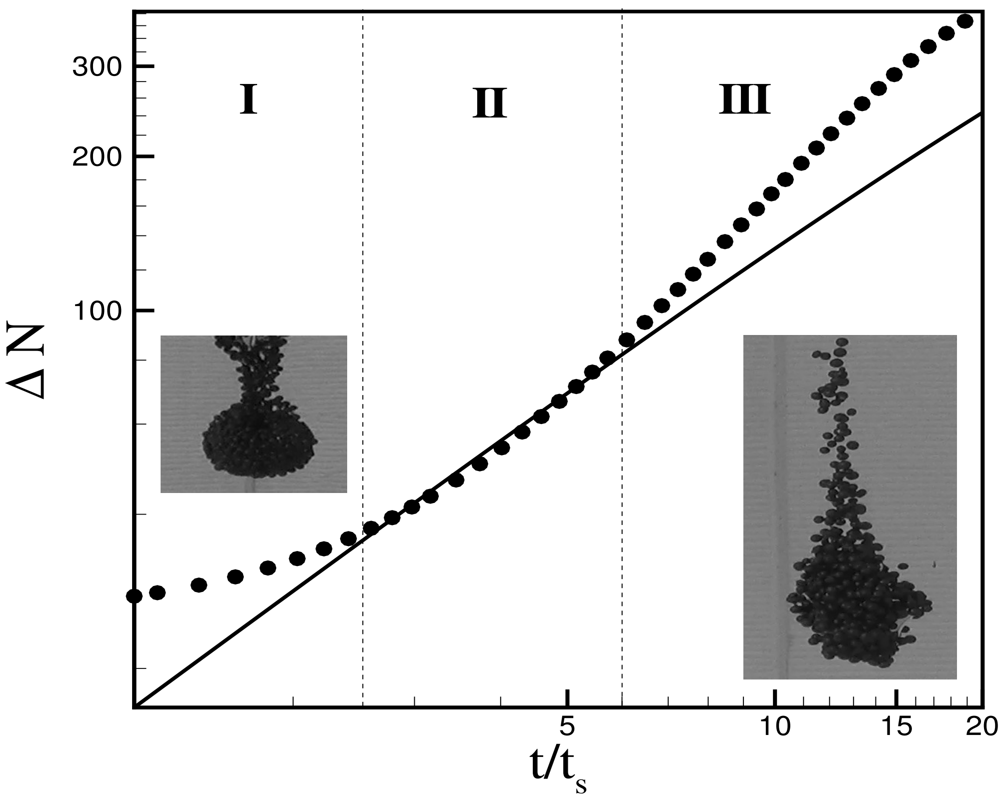

Figure 7: Number of particles that have escaped from the blob as a function of time. The experimental values are represented by the filled circles. The continous line represents the scaling proposed by Abade and Cunha (2007).

(7) is related to hydrodynamic interactions intensity inside the blob it is expected some divergence between experiments and simulations. This divergence occurs due to one main reason.The initial volume fraction of the aggregate is probably smaller in the experiment (leading to lower intensities of particle hydrodynamic interactions in the experiment) and thus the velocity in which the particles escape from the blob is lower in the experiments. We have calculated a magnitude order for constant κ throug equation (11) and obtained $\kappa \approx 0.005$. The value of κ used to fit the experimental values in Fig. 7 is $\kappa \sim 0.006$. This scaling is compatible with our experiments.

Another interesting result is the anisotropy ratio of the blob D, defined as (Taylor and Acrivos, 1964)

$$D = \frac{A - B}{A + B}, \tag{12}$$

where A is the horizontal radius of the blob and B is the vertical radius. For a perfect circle we have $D = 0$. If $D > 0$ the blob is elongated in the horizontal direction, while for $D < 0$ the elongation occurs in the vertical direction. Figure 8 shows the behavior of D as a function of time. It is clear that the initial structure is not an isotropic sphere and resembles an ellipse elongated in the horizontal direction. The details of the initial configuration can be seen in the insert of Fig. 8. After approximately $6.5t_s$ the blob reaches an isotropic pattern for which $D = 0$ and start to elongate vertically ($D < 0$).

After $9t_s$ the anisotropy ratio reaches a value of $D \approx -0.3$. With this elongation the structure cannot maintain itself as a single blob and a sudden particle release occurs. This release leads the anistropy ratio for $D \approx -0.1$. The structure is then gradually enlogated again. When the anistropy ratio reaches $D \approx -0.3$ another particle release occurs. This behavior seems to be repeated periodically. Region **II** highlights the maximum value of $D \approx -0.3$ for which the blob can hold itself as a single structure. Region **III** shows the values of $D \approx -0.1$ for which the blob starts to enlogate itself again.

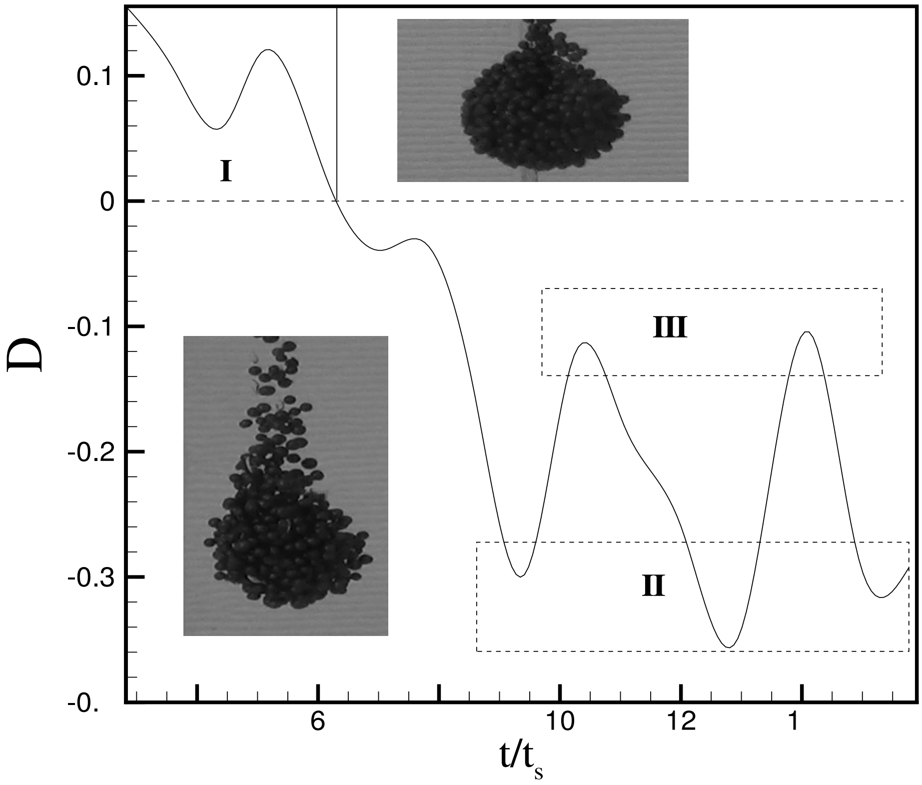

Figure 8: Anisotropy ratio of the blob as a function of time.

5. Conclusions

We have made an experimental and numerical analysis of a sedimenting blob of approximately initially spherical particles immersed in a high viscosity Newtonian liquid. For this purpose an experimental bench was developed in the Vortex Group - Laboratory of Fluid Mechanics. We have used iron particles inside a high viscosity commercial silicon oil. The flow induced by the motion of the particles lies in the Creeping Flow limit where $Re_p \ll 1$. We have also calculated the Stokes number of the particles and have shown that the experiments were made for $St \ll 1$. Under these conditions we used the non commercial research code SIMS written by Gontijo (2013) based on a Mobility formulation (null Stokes number) to provide a qualitative comparision between experiments and numerical simulations.

Several classical features of this problem were captured in this work. For instance we have observed a systematic particle escape from the blob's main strucutre. We argue that this phenomenon is generated due to velocity fluctuations induced by hydrodynamic interactions inside the blob. This behavior was observed both numerically and experimentally. In both cases we have ocasional particles moving to the side edged of the blob. Theses particles end up being captured by the backflow induced by the motion of the blob and as a consequence are moved to its wake. We have also shown the number of particles that escape from the blob as a function of time. Our results fit scaling analysis done in previous works.

Finally we have explored how the shape of the blob vary as a function of time and found out an interesting periodic behavior. This behavior is explained based on the maximum sustainable elongation of the blob. We found out that this elongation leads to a maximum value $|D| \approx 0.3$. For values of $|D| > 0.3$ a sudden particle release from the blob leads these values for $|D| \approx 0.1$. This behavior seems to presents itself as a periodic function of time.

There are still many questions to be explored in future works. We inted to do so and use the knowhow obtained during the production of the present work to explore how other topological changes occur through time and what are the physical mechanisms behind them. We also pretend to explore the problem a sedimenting blob of magnetic particles sedimenting under the presence of an applied field. It is expected that in this problem we could control the motion of the blob and enhance liquid-solid separation velocity in industrial applications.

6. Acknowledgments

The authors would like to thank the undergraduate student in Mechanical Engineering Pedro Henrique Rosa dos Santos from the University of Brasilia for his valuable help with the statistical analysis of the particles used in this work. We would also like to thank CNPq for the finantial support of this work. Grant number: Projeto Universal - 441496/2014-8, CNPq.

References

Abade, G.C. and Cunha, F.R., 2007, *Computer simulation of particle aggregates during sedimentation*, Comput. Methods Appl. Mech. Engrg. 196 (2007) 4597–4612.

Batchelor, G. K., 1972, *Sedimentation in a Dilute Dispersion of Spheres*, J. Fluid Mech., 52, pp. 245-268.

Beenakker, C. W. J., 1986, *Ewald Sum of the Rotne-Prager Tensor*, J. Chem. Phys., 853, pp. 1581-1582.

Boycott, A. E., 1920, *Sedimentation of Blood Corpuscles*, Nature, 104, 532–532.

Brady, J. F. and Durlofsky, L. J., 1988, *The Sedimentation Rate of Disordered Suspensions*, Phys. Fluids, 31(4), pp. 717-727.

Caflisch, R. E. and Luke, J. H. C., 1985, *Variance in the Sedimentation Speed of a Suspension*, Phys. Fluids, 283, 759–760.

Cunha, F. R., Hinch, E.J, 1996, *Shear-induced dispersion in a dilute suspension of rough spheres*, Journal of Fluid Mechanics **309**, 211.

Cunha, F. R., Abade, G. C., Souza, A. J. and Hinch E. J., 2002, *Modeling and Direct Simulation of Velocity Fluctuations and Particle-Velocity Correlations in Sedimentation*, Journals of Fluids Engineering, Vol. 124, pp-957-968.

Cunha, F. R., Gontijo, R. G. and Sobral Y. D., 2013, *Symmetry breaking of particle trajectories due to magnetic interactions in a dilute suspension*, Journals of Magnetism and Magnetic Materials, Vol. 326, pp-240-250.

Davis, R. H., and Acrivos, A., 1985, *Sedimentation of Noncolloidal Particles at Low Reynolds Number*, Annu. Rev. Fluid Mech., **17**(91), pp. 91–118.

Ewald, P. P. 1921, *Die Berechnung Optisher und Elektrostatischer Gitterpotentiale*, Ann. Phys. Lpz., Vol. 64, p. 253.

Gontijo, R.G., 2013, *Micromechanics and Microhydrodynamics of Magnetic Suspensions*, PhD. Thesis, University of Brasília, Brazil, 262 p.

Hasimoto, H., 1959, *On the Periodic Fundamental Solutions of the Stokes Equations and Their Applications to Viscous Flow Past a Cubic Array of Spheres*, J. Fluid Mech., Vol. 5, pp. 317-328.

Hinch, E. J., 1988, *Disorder and Mixing*, Kluwer Academic, Dordrecht, pp. 153âĂŞ161, Chap. 9.

Kim, S. and Karrila, S. J., 2005, *Microhydrodinamics - Principles and Selected Applications*, 2005, Dover Edition, ISBN-13: 978-0486442198.

Ladd, A. J. C., 2002, *Effects of Container Walls on the Velocity Fluctuations of Sedimenting Spheres*, Phys. Rev. Lett. 88, 048301.

Nicolai, H. and Guazzelli, E., 1995, *Effect of the vessel size on the hydrodynamic diffusion of sedimenting spheres*, Phys. Fluids **7**, 3.

Nguyen, N.Q. and Ladd, A. J. C., 2004, *Microstructure in a settling suspension of hard spheres*, Phys. Rev. E 69, 050401 (R).

Richardson, J. F., and Zaki, W. N., 1954, *Sedimentation and Fluidization: I*, Trans. Inst. Chem. Eng., 32, 35–52.

Rotne, J. and Prager, S., 1969, *Variational Treatment of Hydrodynamic Interaction in Polymers*, J. Chem. Phys., 5011, pp. 4831-4837.

Sangani, A. S. and Acrivos, A., 1982, *Slow Flow Through a Periodic Array of Spheres*, Int. J. Multiphase Flow, 84, pp. 343-360.

Taylor, T. D. and Acrivos, A., 1964, *On the deformation of a falling viscous drop at low Reynolds number*, J. Fluid Mech., 18, pp. 466-476.

7. RESPONSIBILITY NOTICE

The authors are the only responsible for the printed material included in this paper.